Pergamon

Int. J. Solids Structures Vol. 32, No. 24, pp. 3603–3628, 1995

0020-7683/95 $9.50 + .00

0020-7683(95)00006-2

INTERFACIAL CIRCULAR CRACK IN CYLINDRICALLY ANISOTROPIC COMPOSITES UNDER ANTIPLANE SHEAR

S. YANG and F. G. YUAN
Department of Mechanical and Aerospace Engineering, North Carolina State University, Raleigh, NC 27695-7910, U.S.A.

(*Received* 12 *August* 1994; *in revised form* 19 *December* 1994)

Abstract—The paper investigates the antiplane shear problem of a dissimilar interfacial circular crack in cylindrically anisotropic composites. Using the theory of analytical functions, a general solution based on a complex variable displacement function is obtained, which is similar to Lekhnitskii's stress potentials for rectilinearly anisotropic material. For some cases, the circular crack problems are reduced to Hilbert problems which are solved in a closed form. The first three-term asymptotic expansions of the near crack-tip stress field are given to identify the role of the curvature effect. The asymptotic solutions are further compared with exact solutions. These solutions show that the leading term exhibits an inverse square root stress singularity regardless of the material properties. In order to compare the stress field near the crack tip for a curved crack with that of a planar crack, a solution for a rectilinearly anisotropic body with a centered straight interfacial crack is also presented.

1. INTRODUCTION

In predicting an accurate stress field near the crack tip under various loading, antiplane shear loading is often considered as a model case since closed form solutions are attainable in some instances. These solutions provide a basis for a qualitative fundamental understanding of the more complicated in-plane loading. Crack problems may be classified into two categories depending on the type of crack geometry considered. The first class of the problems involves planar or straight cracks. The shear tractions acting on the crack surfaces of an infinite solid in homogeneous orthotropic materials under longitudinal shear has been examined by Sih and Chen (1981), using the complex potentials technique introduced by Muskhelishvili (1953). Zhang (1984) investigated a finite body containing an interfacial crack between two isotropic solids under surface-loaded shear tractions using Fourier transform and Fourier series methods. Wu and Chiu (1991) studied the antiplane shear interface crack problem loaded along the boundary of a finite anisotropic body using an integral equation formulation with a boundary collocation method. Recently, a kinked crack in homogeneous media and a kink interfacial crack under uniform crack surface tractions has been studied by Choi and Earmme (1990) and Choi *et al.* (1994) using the Mellin transform and Wiener–Hopf technique.

The second group of the problems involves curved or nonplanar cracks. This class of problems is of particular interest in micromechanics, for predicting fracture between the fiber and the matrix. Sih (1965) derived and solved a circular crack in an infinite homogeneous isotropic body under remote longitudinal shear using a conformal mapping technique. For interfacial curved crack problems, Tamate and Yamada (1969) presented a solution of a partially debonded circular interface crack between inclusion and matrix under remote antiplane shear stresses. Smith (1969) studied a partially debonded interface of a circular inclusion under remote antiplane shear stresses and a debonded surface shear loading using the method of dislocations. Karihaloo and Viswanathan (1985) used an Eshelby's equivalent inclusion method to study an elliptic shaped interface crack between two isotropic materials. The fiber–matrix interfacial crack has been recently addressed by Teng (1992) and Teng and Agah-Tehrani (1993) by considering the interaction between neighboring fibers using a generalized self-consistent scheme and a periodic array model.

In this paper a circular interfacial crack between dissimilar cylindrically anisotropic composites subjected to antiplane shear is presented. In the next section, the basic equations of cylindrically anisotropic elasticity under antiplane shear are formulated based on a complex variable displacement function. A general solution for the stress and displacement in a cylindrically anisotropic composite is established in Section 2. The solution of constant shear tractions acting on the interface for both regions with material anisotropy is considered in Section 3. Another example which simulates the anisotropic fiber imbedded in an isotropic matrix is studied. The derivation and solution of an interfacial circular crack under remote antiplane shear stresses are examined. In this paper, asymptotic solutions up to the third-term expansion are derived to elucidate the role of curvature on the angular distributions of stresses near the crack tips. For comparison of the crack-tip stress field between circular and straight cracks, a planar interfacial crack between dissimilar rectilinearly anisotropic solids under constant surface shear tractions is derived and discussed in the Appendix.

2. MATHEMATICAL FORMULATION

Consider a cylindrically anisotropic elastic body deformed under antiplane shear. The strain–displacement, stress–strain, and the equilibrium equation in the absence of body force are given by

$$\gamma_{rz} = \frac{\partial w}{\partial r} \quad \gamma_{\theta z} = \frac{1}{r}\frac{\partial w}{\partial \theta} \tag{1}$$

$$\tau_{\theta z} = C_{44}\gamma_{\theta z} + C_{45}\gamma_{rz} \quad \tau_{rz} = C_{45}\gamma_{\theta z} + C_{55}\gamma_{rz} \tag{2}$$

$$\frac{\partial \tau_{rz}}{\partial r} + \frac{1}{r}\frac{\partial \tau_{\theta z}}{\partial \theta} + \frac{\tau_{rz}}{r} = 0 \tag{3}$$

where $w(r, \theta)$ is the displacement in a direction perpendicular to the x–y plane, $\gamma_{\beta z}$ and $\tau_{\beta z}$ are strain and stress components, respectively. C_{ij} are the stiffness coefficients.

Substituting eqns (1) and (2) into eqn (3), the equilibrium equation can be written as

$$C_{55}\left(\frac{\partial^2 w}{\partial r^2} + \frac{1}{r}\frac{\partial w}{\partial r}\right) + 2C_{45}\frac{1}{r}\frac{\partial^2 w}{\partial r \partial \theta} + C_{44}\frac{1}{r^2}\frac{\partial^2 w}{\partial \theta^2} = 0. \tag{4}$$

A general solution of eqn (4) which is similar to Lekhnitskii's (1963) complex variable stress potentials in the rectilinearly anisotropic material can be expressed as

$$w(r, \theta) = 2\,\mathrm{Re}\,[W(z_3)] \tag{5}$$

where a new argument z_3 is defined as

$$z_3 = \left(\frac{r}{a}\right)^{-i\lambda - 1} \mathrm{re}^{i\theta} \tag{6}$$

where a is a characteristic length designated here as the radius of the circular arc. The λ are roots of the following algebraic characteristic equation

$$C_{55}\lambda^2 - 2C_{45}\lambda + C_{44} = 0. \tag{7}$$

When the material is isotropic, λ becomes i. The roots of eqn (7) are either complex or pure imaginary but cannot be real. Without loss of generality, λ is chosen as

$$\lambda = [C_{45} + i\sqrt{C_{44}C_{55} - C_{45}^2}]/C_{55}$$

where $\mathrm{Re}(-i\lambda) = \sqrt{C_{44}C_{55} - C_{45}^2}/C_{55} > 0$. It is convenient to introduce a function

$$\Phi(z_3) = \sqrt{C_{44}C_{55} - C_{45}^2}\, z_3 \frac{\mathrm{d}W(z_3)}{\mathrm{d}z_3} \tag{8}$$

so that stress components can be simply written as

$$\tau_{rz} = \frac{2}{r}\mathrm{Re}[\Phi(z_3)] \quad \tau_{\theta z} = \frac{2}{r}\mathrm{Re}[\lambda\Phi(z_3)] \tag{9}$$

and

$$\frac{\partial w}{\partial \theta} = \frac{i}{\mu}[\Phi(z_3) - \bar{\Phi}(\bar{z}_3)] \tag{10}$$

where $\mu = \sqrt{C_{44}C_{55} - C_{45}^2}$ and a bar denotes a complex conjugate.

Having established the general solution for the stress and displacement in a cylindrically anisotropic material, we can study the interfacial curved crack between dissimilar cylindrically anisotropic materials in the next section.

3. INTERFACE CRACK BETWEEN DISSIMILAR CYLINDRICALLY ANISOTROPIC MATERIALS

Consider a circular crack lying along the interface of two cylindrically anisotropic elastic solids, subtending an angle 2α at the center of the circle as shown in Fig. 1. Further, let equal and opposite known tractions $\tau(a\,e^{i\theta})$ be applied to each crack surface. Then the boundary conditions along $z = a\,e^{i\theta}$ are

$$\frac{\partial w^{(1)}}{\partial \theta} = \frac{\partial w^{(2)}}{\partial \theta} \quad \tau_{rz}^{(1)} = \tau_{rz}^{(2)} \quad \text{on } |z| = a, \quad |\theta| > \alpha \tag{11}$$

and

$$\tau_{rz}^{(1)} = \tau(a\,e^{i\theta}) \quad \tau_{rz}^{(2)} = \tau(a\,e^{i\theta}) \quad \text{on } |z| = a, \quad |\theta| < \alpha. \tag{12}$$

Here, and in the sequel, the superscripts or subscripts 1 and 2 denote the internal and

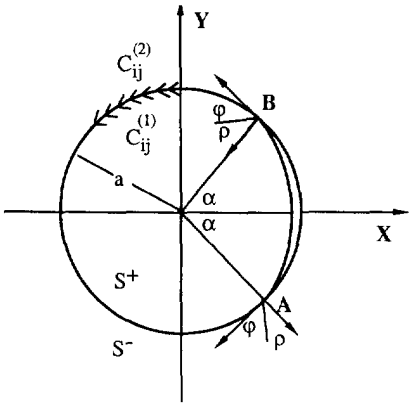

Fig. 1. Geometry and coordinates of an interfacial curved crack between cylindrically anisotropic materials.

external materials respectively. From eqns (9) and (10), the conditions (11) and (12) can be rewritten in the form

$$\begin{aligned} &\frac{1}{\mu_1}[\Phi_1(z)-\bar{\Phi}_1(\bar{z})] = \frac{1}{\mu_2}[\Phi_2(z)-\bar{\Phi}_2(\bar{z})] \\ &\Phi_1(z)+\Phi_1(\bar{z}) = \Phi_2(z)+\bar{\Phi}_2(\bar{z}) \end{aligned} \quad \text{on } |z| = a, |\theta| > \alpha \tag{13}$$

$$\begin{aligned} &\Phi_1(z)+\bar{\Phi}_1(\bar{z}) = \frac{a}{2}\tau(z) \\ &\Phi_2(z)+\bar{\Phi}_2(\bar{z}) = \frac{a}{2}\tau(z) \end{aligned} \quad \text{on } |z| = a, |\theta| < \alpha. \tag{14}$$

where $\bar{z} = a^2/z$. The following two cases are considered in this paper.

Crack under surface traction

For the case of constant surface traction $\tau(z) = -\tau_0$ with zero stresses at infinity, it readily follows from eqn (13) that

$$\begin{aligned} &\frac{1}{\mu_1}\Phi_1(z)+\frac{1}{\mu_2}\Phi_2\left(\frac{a^2}{z}\right) = \frac{1}{\mu_2}\Phi_2(z)+\frac{1}{\mu_1}\bar{\Phi}_1\left(\frac{a^2}{z}\right) \\ &\Phi_1(z)-\bar{\Phi}_2\left(\frac{a^2}{z}\right) = \Phi_2(z)-\bar{\Phi}_1\left(\frac{a^2}{z}\right) \end{aligned} \quad \text{on } |z| = a, \quad |\theta| > \alpha.$$

Defining two new functions

$$\begin{aligned} &\frac{1}{\mu_1}\Phi_1(z)+\frac{1}{\mu_2}\bar{\Phi}_2\left(\frac{a^2}{z}\right) \equiv \Psi(z) \quad z \in S^+ \\ &\frac{1}{\mu_2}\Phi_2(z)+\frac{1}{\mu_1}\bar{\Phi}_1\left(\frac{a^2}{z}\right) \equiv \Psi(z) \quad z \in S^- \end{aligned} \tag{15}$$

$$\begin{aligned} &\Phi_1(z)-\bar{\Phi}_2\left(\frac{a^2}{z}\right) \equiv \Theta(z) \quad z \in S^+ \\ &\Phi_2(z)-\Phi_1\left(\frac{a^2}{z}\right) \equiv \Theta(z) \quad z \in S^- \end{aligned} \tag{16}$$

then the displacements and stresses described by Ψ and Θ are continuous across the interface. In eqns (15) and (16), $\Psi(z)$ and $\Theta(z)$ are analytic functions in the whole plane cut along the arc $r = a$, $|\theta| < \alpha$, with the possible exclusion of the origin and infinity. Note that S^+ and S^- are the inner and outer regions respectively. Based on the definition of eqns (15) and (16), we have

$$\bar{\Psi}\left(\frac{a^2}{z}\right) = \Psi(z) \quad \bar{\Theta}\left(\frac{a^2}{z}\right) = -\Theta(z) \quad z \in S^+ \text{ and } S^-. \tag{17}$$

Solving eqns (15) and (16) for $\Phi_1(z)$ and $\Phi_2(z)$, we obtain

$$\Phi_1(z) = \frac{\mu_1\mu_2}{\mu_1+\mu_2}\left[\Psi(z)+\frac{\Theta(z)}{\mu_2}\right], \quad \bar{\Phi}_2\left(\frac{a^2}{z}\right) = \frac{\mu_1\mu_2}{\mu_1+\mu_2}\left[\Psi(z)-\frac{\Theta(z)}{\mu_1}\right] \quad z\in S^+$$

$$\Phi_2(z) = \frac{\mu_1\mu_2}{\mu_1+\mu_2}\left[\Psi(z)+\frac{\Theta(z)}{\mu_1}\right], \quad \bar{\Phi}_1\left(\frac{a^2}{z}\right) = \frac{\mu_1\mu_2}{\mu_1+\mu_2}\left[\Psi(z)-\frac{\Theta(z)}{\mu_2}\right] \quad z\in S^-. \tag{18}$$

Substituting eqn (18) into the remaining condition (12) yields

$$\begin{aligned}
&\Psi^+(z)+\Psi^-(z)+\frac{1}{\mu_2}[\Theta^+(z)-\Theta^-(z)] = \frac{\mu_1+\mu_2}{\mu_1\mu_2}a\tau(z)\\
&\Psi^+(z)+\Psi^-(z)-\frac{1}{\mu_1}[\Theta^+(z)-\Theta^-(z)] = \frac{\mu_1+\mu_2}{\mu_1\mu_2}a\tau(z)
\end{aligned} \quad \text{on } |z| = a, \quad |\theta| < \alpha \tag{19}$$

that is,

$$\Theta^+(z)-\Theta^-(z) = 0 \quad \Psi^+(z)+\Psi^-(z) = \frac{\mu_1+\mu_2}{\mu_1\mu_2}a\tau(z) \quad \text{on } |z| = a, \quad |\theta| < \alpha \tag{20}$$

where Ψ^+, Θ^+ and Ψ^-, Θ^- are the limiting values of the functions approaching from S^+ and S^- to the crack surfaces respectively. The unknown functions $\Psi(z)$ and $\Theta(z)$ are governed by eqns (20), which are a pair of Hilbert problems. The solutions for eqns (20) have been given by Muskhelishvili (1953) as

$$\Theta(z) = P(z) \tag{21}$$

$$\Psi(z) = \frac{1}{2\pi i}\frac{\mu_1+\mu_2}{\mu_1\mu_2}a\chi_0(z)\int_L \frac{\tau(t)\,dt}{\chi_0^+(t)(t-z)} + \chi_0(z)R(z) \tag{22}$$

where $P(z)$ and $R(z)$ are holomorphic functions in the whole plane except possibly at the origin and infinity; L is the arc $|z| = a$, $|\theta| < \alpha$, and

$$\chi_0(z) = (z-a\,e^{i\alpha})^{-1/2}(z-a\,e^{-i\alpha})^{-1/2}.$$

With $\tau(z) = -\tau_0 =$ constant along the crack surface, Ψ can be simplified as

$$\Psi(z) = -\frac{\mu_1+\mu_2}{2\mu_1\mu_2}\tau_0 a[1+(a\cos\alpha-z)\chi_0(z)]+\chi_0(z)R(z). \tag{23}$$

By replacing the argument z of functions $\Theta(z)$ and $\Psi(z)$ by z_3 in eqns (21) and (23), the complete functions of $\Theta(z_3)$ and $\Psi(z_3)$ can be obtained. If the body is taken to be infinite in extent and the stresses are assumed to vanish at infinity, it is sufficient to assume

$$\Theta(z_3) = \sum_{k=-1}^{1} D_k z_3^k \quad R(z_3) = \sum_{k=-1}^{2} C_k z_3^k \tag{24}$$

From eqns (9) and (18), we have

$$\begin{aligned}
\tau_{rz}^{(1)} &= \frac{2}{r}\frac{\mu_1\mu_2}{\mu_1+\mu_2}\mathrm{Re}\left[\left(\Psi(z_3)+\frac{\Theta(z_3)}{\mu_2}\right)\right]\\
\tau_{\theta z}^{(1)} &= \frac{2}{r}\frac{\mu_1\mu_2}{\mu_1+\mu_2}\mathrm{Re}\left[\lambda_1\left(\Psi(z_3)+\frac{\Theta(z_3)}{\mu_2}\right)\right]
\end{aligned} \tag{25}$$

$$\tau_{rz}^{(2)} = \frac{2}{r}\frac{\mu_1\mu_2}{\mu_1+\mu_2}\mathrm{Re}\left[\left(\Psi(z_3)+\frac{\Theta(z_3)}{\mu_1}\right)\right]$$

$$\tau_{\theta z}^{(2)} = \frac{2}{r}\frac{\mu_1\mu_2}{\mu_1+\mu_2}\mathrm{Re}\left[\lambda_2\left(\Psi(z_3)+\frac{\Theta(z_3)}{\mu_1}\right)\right] \tag{26}$$

Since $\mathrm{Re}(-i\lambda_k) > 0$, $\lim_{r\to 0}|z_3| = 0$ and $\lim_{r\to\infty}|z_3| \to \infty$. Moreover, when the center of the internal region is approached, anisotropic material occupies the central portion of the region, thereby $\lambda_1 \to i$ as $r \to 0$. On examining the stresses at the origin and infinity, we find

$$-C_{-1} + \frac{a}{\mu_2}D_{-1} = 0$$

$$C_0 + \frac{\cos\alpha}{a}C_{-1} - \frac{a}{\mu_2}D_0 = -\frac{\mu_1+\mu_2}{2\mu_1\mu_2}\tau_0 a^2(1-\cos\alpha)$$

$$C_2 + \frac{D_1}{\mu_1} = 0. \tag{27}$$

From eqn (17) and the condition of a single-valued displacement field, we have

$$\bar{C}_2 a^2 + \frac{C_{-1}}{a} = 0$$

$$\bar{C}_1 a + C_0 = -\frac{\mu_1+\mu_2}{2\mu_1\mu_2}\tau_0 a^2(1-\cos\alpha)$$

$$D_0 = -\bar{D}_0, \quad D_{-1} + \bar{D}_1 a^2 = 0$$

$$\mathrm{Im}(D_0) = 0. \tag{28}$$

The solutions to eqns (27) and (28) are

$$C_0 = -\frac{\mu_1+\mu_2}{2\mu_1\mu_2}\tau_0 a^2(1-\cos\alpha)$$

$$C_{-1} = C_1 = C_2 = D_{-1} = D_0 = D_1 = 0.$$

Thus we get

$$\Theta(z_3) = 0 \quad \Psi(z_3) = -\frac{\mu_1+\mu_2}{2\mu_1\mu_2}\tau_0 a[1+(a-z_3)\chi_0(z_3)]. \tag{29}$$

From eqns (25), (26) and (29), the entire stress field can be found. Expanding $\Psi(z_3)$ for a small distance ρ from the crack tips, $z = a\,e^{\pm i\alpha}$, and keeping terms up to the order of $O(\sqrt{\rho})$, the first three-term asymptotic expansions of the crack-tip stress field are

$$\tau_{\gamma z}^{(k)} = \sum_{i=1}^{3} A_i \rho^{s_i}\tilde{\tau}_{\gamma z_k}^{(i)}(\varphi) \quad \gamma = r, \theta, \quad k = 1, 2 \tag{30}$$

where $s_1 = -\frac{1}{2}, s_2 = 0, s_3 = \frac{1}{2}$

$$A_1 = \tau_0\sqrt{\frac{2a}{\sin\alpha}}\sin\frac{\alpha}{2}, \quad A_2 = -\tau_0, \quad A_3 = \tau_0\sqrt{\frac{1}{2a\sin\alpha}}$$

$$\tilde{\tau}^{(1)}_{rz_k} = \mathrm{Re}\left[\frac{1}{\sqrt{\cos\varphi+\lambda_k\sin\varphi}}\right], \quad \tilde{\tau}^{(2)}_{rz_k} = 1, \quad \tilde{\tau}^{(3)}_{rz_k} = \mathrm{Re}\,[\Phi_{3k}]$$

$$\tilde{\tau}^{(1)}_{\theta z_k} = \mathrm{Re}\left[\frac{\lambda_k}{\sqrt{\cos\varphi+\lambda_k\sin\varphi}}\right], \quad \tilde{\tau}^{(2)}_{\theta z_k} = \mathrm{Re}\,[\lambda_k], \quad \tilde{\tau}^{(3)}_{\theta z_k} = \mathrm{Re}\,[\lambda_k\Phi_{3k}]$$

$$\Phi_{3k} = \frac{\pm 2\sin\varphi\sin\frac{\alpha}{2}}{\sqrt{\cos\varphi+\lambda_k\sin\varphi}} \pm \frac{i(i-\lambda_k)\sin\frac{\alpha}{2}}{2(\cos\varphi+\lambda_k\sin\varphi)^{3/2}}(\lambda_k\sin^2\varphi + i\cos^2\varphi + \sin 2\varphi)$$
$$+\sqrt{(\cos\varphi+\lambda_k\sin\varphi)}\left(e^{\pm i\frac{\alpha}{2}} - \frac{e^{\pm i\alpha}}{4\cos\frac{\alpha}{2}}\right) \quad \text{near } B, A = ae^{\pm i\alpha}$$

and the quantities with $(\sim)$ represent their angular distributions.

Using stress transformations,

$$\left.\begin{aligned}\tau_{\rho z} &= \pm\tau_{\theta z}\cos(\varphi\pm\alpha-\theta) \mp \tau_{rz}\sin(\varphi\pm\alpha-\theta)\\ \tau_{\varphi z} &= \mp\tau_{\theta z}\sin(\varphi\pm\alpha-\theta) \mp \tau_{rz}\cos(\varphi\pm\alpha-\theta)\end{aligned}\right\} \quad \text{near } B, A = ae^{\pm i\alpha} \tag{31}$$

we have

$$\tau^{(k)}_{\gamma z} = \mp\sum_{i=1}^{3} A_i\rho^{\nu_i}\tilde{\tau}^{(i)}_{\gamma z_k}(\varphi) \quad \gamma = \rho, \varphi \quad \text{near } B, A = ae^{\pm i\alpha} \tag{32}$$

where

$$\tilde{\tau}^{(1)}_{\rho z_k} = \mathrm{Re}\left[\frac{\sin\varphi-\lambda_k\cos\varphi}{\sqrt{\cos\varphi+\lambda_k\sin\varphi}}\right], \quad \tilde{\tau}^{(1)}_{\varphi z_k} = \mathrm{Re}[\sqrt{\cos\varphi+\lambda_k\sin\varphi}]$$

$$\tilde{\tau}^{(2)}_{\rho z_k} = \mathrm{Re}\,[\sin\varphi-\lambda_k\cos\varphi], \quad \tilde{\tau}^{(2)}_{\varphi z_k} = \mathrm{Re}\,[\cos\varphi+\lambda_k\sin\varphi] \tag{33}$$

$$\left.\begin{aligned}\tilde{\tau}^{(3)}_{\rho z_k} &= \mathrm{Re}\left[(\sin\varphi-\lambda_k\cos\varphi)\Phi_{3k} \mp 2\sqrt{\cos\varphi+\lambda_k\sin\varphi}\cos\varphi\sin\frac{\alpha}{2}\right]\\ \tilde{\tau}^{(3)}_{\varphi z_k} &= \mathrm{Re}\left[(\cos\varphi+\lambda_k\sin\varphi)\Phi_{3k} \pm 2\frac{\sin\varphi-\lambda_k\cos\varphi}{\sqrt{\cos\varphi+\lambda_k\sin\varphi}}\cos\varphi\sin\frac{\alpha}{2}\right]\end{aligned}\right\} \quad \text{near } B, A = ae^{\pm i\alpha}.$$

When $a \to \infty$, with the length $2a\alpha$ being kept constant, the curved crack approaches a planar crack and the cylindrical anisotropy approaches the rectilinear anisotropy. The asymptotic solution of the near crack-tip stress fields up to the third-term expansion is

$$\tau^{(k)}_{\gamma z} = \mp\sum_{i=1}^{3} B_i\rho^{\nu_i}\tilde{\tau}^{(i)}_{\gamma z_k}(\varphi) \quad \gamma = \rho, \varphi \quad \text{near } B, A = ae^{\pm i\alpha} \tag{34}$$

where

$$B_1 = \lim_{\substack{a\to\infty \\ a\alpha = \text{const}}} A_1 = \tau_0\sqrt{\frac{a\alpha}{2}} \quad B_2 = \lim_{\substack{a\to\infty \\ a\alpha = \text{const}}} A_2 = -\tau_0 \quad B_3 = \lim_{\substack{a\to\infty \\ a\alpha = \text{const}}} A_3 = \tau_0\sqrt{\frac{1}{2a\alpha}} \tag{35}$$

and $\tilde{\tau}^{(i)}_{\rho z_k}, \tilde{\tau}^{(i)}_{\varphi z_k}, i = 1, 2$ remain the same as those of curved crack given by eqn (33), while

$$\tilde{\tau}^{(3)}_{\rho z_k} = \mathrm{Re}\left[\tfrac{3}{4}(\sin\varphi - \lambda_k\cos\varphi)\sqrt{\cos\varphi + \lambda_k\sin\varphi}\right]$$

$$\tilde{\tau}^{(3)}_{\varphi z_k} = \mathrm{Re}\left[\tfrac{3}{4}(\cos\varphi + \lambda_k\sin\varphi)^{3/2}\right].$$

Note that the length of the planar crack is $2a\alpha$ in eqn (35).

Comparing the stress field for the curved crack [eqn (32)] with the case for the planar crack [eqn (34)], it is clear that both the stress fields have identical angular distributions for the first two-terms, but the angular distributions for the third term are different in the two cases. A relevant problem of rectilinearly anisotropic solids with interfacial cracks under surface tractions shown in Fig. 2 is derived and compared in the Appendix.

The singular term for both circular and planar cracks can be written in the form

$$\tau^{(k)}_{rz} = \frac{K_{\mathrm{III}}}{\sqrt{2\pi\rho}}\,\mathrm{Re}\left[\frac{1}{\sqrt{\cos\varphi + \lambda_k\sin\varphi}}\right] \quad \tau^{(k)}_{\theta z} = \frac{K_{\mathrm{III}}}{\sqrt{2\pi\rho}}\,\mathrm{Re}\left[\frac{\lambda_k}{\sqrt{\cos\varphi + \lambda_k\sin\varphi}}\right] \tag{36}$$

where K_{III} is the stress intensity factor, and

$$K^{\mathrm{c}}_{\mathrm{III}} = \tau_0\sqrt{2a\pi\tan\frac{\alpha}{2}} = \frac{\tau_0\sqrt{a\pi\sin\alpha}}{\cos\frac{\alpha}{2}} = \sqrt{2\pi}A_1 \quad \text{for a curved crack}$$

$$K^{\mathrm{s}}_{\mathrm{III}} = \lim_{\substack{a\to\infty \\ a\alpha = \text{const}}} K^{\mathrm{c}}_{\mathrm{III}} = \tau_0\sqrt{\pi a\alpha} = \sqrt{2\pi}B_1 \quad \text{for a planar crack.} \tag{37}$$

The superscripts c and s stand for the quantities associated with a circular and a planar crack respectively. If both the inner and outer materials are isotropic, the leading term of eqn (30) coincides with that given by Smith (1969).

Crack under uniform shear stresses at infinity

At infinity, the body is subjected to uniform shear stresses $\underset{|z|\to\infty}{\tau_{xz}} = \tau^{\infty}_x$, $\underset{|z|\to\infty}{\tau_{yz}} = \tau^{\infty}_y$, which make an angle β with the x-axis, and the surface is free of tractions. It readily follows from eqn (14) that

$$\Phi_1(z) = -\overline{\Phi}_1\left(\frac{a^2}{z}\right) \quad \Phi_2(z) = -\overline{\Phi}_2\left(\frac{a^2}{z}\right) \quad \text{on } |z| = a, \quad |\theta| < \alpha. \tag{38}$$

Thus if we define the two new functions as

$$\begin{aligned}
\Phi_1(z) &\equiv \Psi(z) \quad z\in S^+ \\
-\overline{\Phi}_1\left(\frac{a^2}{z}\right) &\equiv \Psi(z) \quad z\in S^- \\
\Phi_2(z) &\equiv \Theta(z) \quad z\in S^- \\
-\overline{\Phi}_2\left(\frac{a^2}{z}\right) &\equiv \Theta(z) \quad z\in S^+
\end{aligned} \tag{39}$$

then the condition of traction-free on the crack surfaces is satisfied. In eqn (39) $\Psi(z)$ and $\Theta(z)$ are analytic functions in the whole plane cut along the arc $r = a$, $|\theta| < \alpha$, with the possible exclusion of the origin and infinity. Based on the definition in eqn (39), we have

$$\overline{\Psi}\left(\frac{a^2}{z}\right) = -\Psi(z) \quad \overline{\Theta}\left(\frac{a^2}{z}\right) = -\Theta(z) \quad z \in S^+ \text{ and } S^-. \tag{40}$$

Using eqn (39), condition (13) can alternatively be written as

$$\frac{\Psi^+(z)}{\mu_1} - \frac{\Theta^+(z)}{\mu_2} + \left[\frac{\Psi^-(z)}{\mu_1} - \frac{\Theta^-(z)}{\mu_2}\right] = 0 \tag{41}$$

$$|z| = a, |\theta| > \alpha$$

$$\Psi^+(z) + \Theta^+(z) - [\Psi \quad (z) + \Theta \quad (z)] = 0. \tag{42}$$

The unknown functions $\Psi(z)$ and $\Theta(z)$ are governed by eqns (41) and (42) which are a pair of Hilbert problems. The solution to eqns (41) and (42) can be expressed as

$$\Psi(z) + \Theta(z) = P(z) \quad \frac{\Psi(z)}{\mu_1} - \frac{\Theta(z)}{\mu_2} = \chi_0(z) R(z) \tag{43}$$

where

$$P(z) = \sum_{k=-1}^{1} D_k z^k \quad R(z) = \sum_{k=-1}^{2} C_k z^k$$

$$\chi_0(z) = (z - a e^{i\alpha})^{-1/2} (z - a e^{-i\alpha})^{-1/2}.$$

Solving eqns (43) for $\Theta(z)$ and $\Psi(z)$ yields

$$\Psi(z) = \frac{\mu_1 \mu_2}{\mu_1 + \mu_2}\left[\frac{P(z)}{\mu_2} + \chi_0(z) R(z)\right]$$

$$\Theta(z) = \frac{\mu_1 \mu_2}{\mu_1 + \mu_2}\left[\frac{P(z)}{\mu_1} - \chi_0(z) R(z)\right]. \tag{44}$$

Replacing the argument z of functions $\Psi(z)$, $\Theta(z)$ by z_3 and using eqns (9), (39) and (44), the stresses can be expressed in the form

$$\tau_{rz}^{(1)} = \frac{2}{r} \frac{\mu_1 \mu_2}{\mu_1 + \mu_2} \operatorname{Re}\left[\frac{P(z_3)}{\mu_2} + \chi_0(z_3) R(z_3)\right]$$

$$\tau_{\theta z}^{(1)} = \frac{2}{r} \frac{\mu_1 \mu_2}{\mu_1 + \mu_2} \operatorname{Re}\left\{\lambda_1\left[\frac{P(z_3)}{\mu_2} + \chi_0(z_3) R(z_3)\right]\right\} \tag{45}$$

$$\tau_{rz}^{(2)} = \frac{2}{r} \frac{\mu_1 \mu_2}{\mu_1 + \mu_2} \operatorname{Re}\left[\frac{P(z_3)}{\mu_1} - \chi_0(z_3) R(z_3)\right]$$

$$\tau_{\theta z}^{(2)} = \frac{2}{r} \frac{\mu_1 \mu_2}{\mu_1 + \mu_2} \operatorname{Re}\left\{\lambda_2\left[\frac{P(z_3)}{\mu_1} - \chi_0(z_3) R(z_3)\right]\right\}. \tag{46}$$

Further assume the external matrix material is isotropic, that is, $\lambda_2 = i$ and $z_3 = z$ for $z \in S^-$. On examining the stress at origin and infinity, we find

$$\frac{D_{-1}}{\mu_2} + \frac{C_{-1}}{a} = 0$$

$$\frac{D_0}{\mu_2} + \frac{C_0}{a} + \frac{\cos\alpha}{a^2} C_{-1} = 0$$

$$\frac{D_1}{\mu_1} - C_2 = \frac{\mu_1 + \mu_2}{2\mu_1\mu_2} \tau_0 \, e^{-i\beta} \tag{47}$$

where $\tau_0 = \sqrt{(\tau_x^\infty)^2 + (\tau_y^\infty)^2}$, $\tau_0 \cos\beta = \tau_x^\infty$, $\tau_0 \sin\beta = \tau_y^\infty$.

From eqns (40) and the condition of single-valued displacement, we get

$$\frac{D_{-1}}{\mu_2} + \frac{C_{-1}}{a} = -\frac{\bar{D}_1}{\mu_2} a^2 - \bar{C}_2 a^2$$

$$\frac{D_0}{\mu_2} + \frac{C_0}{a} + \frac{\cos\alpha}{a^2} C_{-1} = -\frac{\bar{D}_0}{\mu_2} - \bar{C}_1 - \bar{C}_2 a \cos\alpha$$

$$\frac{D_{-1}}{\mu_2} - \frac{C_{-1}}{a} = -\frac{\bar{D}_1}{\mu_2} a^2 + \bar{C}_2 a^2$$

$$\frac{D_0}{\mu_1} - \frac{C_0}{a} - \frac{\cos\alpha}{a^2} C_{-1} = -\frac{\bar{D}_0}{\mu_1} + \bar{C}_1 + \bar{C}_2 a \cos\alpha$$

$$\mathrm{Im}\,(D_0) = 0. \tag{48}$$

Solving eqns (47) and (48) for C_k and D_k, we find

$$D_1 = \frac{\tau_0}{2} e^{-i\beta} \quad D_{-1} = -\frac{\tau_0}{2} a^2 e^{i\beta} \quad D_0 = 0$$

$$C_{-1} = \frac{\tau_0 a^3}{2\mu_2} e^{i\beta} \quad C_0 = -\frac{\tau_0}{2\mu_2} a^2 e^{i\beta} \cos\alpha \quad C_1 = \frac{\tau_0}{2\mu_2} a e^{-i\beta} \cos\alpha \quad C_2 = -\frac{\tau_0}{2\mu_2} e^{-i\beta}. \tag{49}$$

This leads to the stress solution

$$\tau_{rz}^{(k)} = \frac{\tau_0 a}{(\mu_1 + \mu_2) r} \mathrm{Re} \left\{ \begin{array}{l} \mu_k \left(\dfrac{z_3}{a} e^{-i\beta} - \dfrac{a}{z_3} e^{i\beta} \right) \\ -\mu_1 a \chi_0(z_3) \left[\left(\dfrac{a}{z_3} - \cos\alpha \right) e^{i\beta} + \dfrac{z_3}{a} \left(\cos\alpha - \dfrac{z_3}{a} \right) e^{-i\beta} \right] \end{array} \right\}$$

$$\tau_{\theta z}^{(k)} = \frac{\tau_0 a}{(\mu_1 + \mu_2) r} \mathrm{Re} \left\{ \begin{array}{l} \lambda_k \mu_k \left(\dfrac{z_3}{a} e^{-i\beta} - \dfrac{a}{z_3} e^{i\beta} \right) \\ -\lambda_k \mu_1 a \chi_0(z_3) \left[\left(\dfrac{a}{z_3} - \cos\alpha \right) e^{i\beta} + \dfrac{z_3}{a} \left(\cos\alpha - \dfrac{z_3}{a} \right) e^{-i\beta} \right] \end{array} \right\}$$

where $(z_3)_k$ is abbreviated as z_3. Expanding the stress field for small values of ρ from the crack tips, the first three-term asymptotic expansions of the crack-tip stress field can be expressed as

$$\tau_{\gamma z}^{(k)} = \sum_{i=1}^{3} A_i \rho^{s_i} \tilde{\tau}_{\gamma z_k}^{(i)}(\varphi) \quad \gamma = r, \theta, \quad k = 1, 2 \tag{50}$$

where $s_1 = -\frac{1}{2}, s_2 = 0, s_3 = \frac{1}{2}$

$$\tilde{\tau}_{rz_k}^{(1)} = \mathrm{Re}\left[\frac{1}{\sqrt{\cos\varphi + \lambda_k \sin\varphi}}\right] \qquad \tilde{\tau}_{\theta z_k}^{(1)} = \mathrm{Re}\left[\frac{\lambda_k}{\sqrt{\cos\varphi + \lambda_k \sin\varphi}}\right]$$

$$\tilde{\tau}_{rz_k}^{(2)} = 0 \qquad \tilde{\tau}_{\theta z_k}^{(2)} = \frac{\mu_k}{\sqrt{\mu_1 \mu_2}} \mathrm{Re}\left[-i\lambda_k\right]$$

$$\tilde{\tau}_{rz_k}^{(3)} = \mathrm{Re}\left[\Phi_{3k}\right] \qquad \tilde{\tau}_{\theta z_k}^{(3)} = \mathrm{Re}\left[\lambda_k \Phi_{3k}\right]$$

$$\Phi_{3k} = \frac{\pm \sin\varphi \sin\alpha}{\sqrt{\cos\varphi + \lambda_k \sin\varphi}} \pm \frac{i(i - \lambda_k)\sin\alpha}{4(\cos\varphi + \lambda_k \sin\varphi)^{3/2}} (\lambda_k \sin^2\varphi + i\cos^2\varphi + \sin 2\varphi)$$
$$+ \frac{\sqrt{\cos\varphi + \lambda_k \sin\varphi}}{2} \left[\frac{2\cos(\beta \mp \frac{3}{2}\alpha) \pm i \sin\alpha\, \mathrm{e}^{-i(\beta \mp \alpha/2)}}{\cos\left(\beta \mp \frac{\alpha}{2}\right)} - \frac{\mathrm{e}^{\pm i\alpha}}{2}\right] \quad \text{near } B, A = a\mathrm{e}^{\pm i\alpha}$$

$$\left.\begin{aligned} A_1 &= -\frac{\mu_1 \tau_0}{\mu_1 + \mu_2} \sqrt{2a \sin\alpha} \cos\left(\beta \mp \frac{\alpha}{2}\right) \\ A_2 &= \frac{2\tau_0 \sqrt{\mu_1 \mu_2}}{\mu_1 + \mu_2} \sin(\beta \mp \alpha) \\ A_3 &= \frac{\mu_1 \tau_0}{\mu_1 + \mu_2} \sqrt{\frac{2}{a \sin\alpha}} \cos\left(\beta \mp \frac{\alpha}{2}\right) \end{aligned}\right\} \quad \text{near } B, A = a\mathrm{e}^{\pm i\alpha}.$$

Using stress transformation in eqns (31), we obtain

$$\tau_{\gamma z}^{(k)} = \mp \sum_{i=1}^{3} A_i \rho^{s_i} \tilde{\tau}_{\gamma z_k}^{(i)}(\varphi) \quad \gamma = \rho, \varphi, \quad \text{near } B, A = a\mathrm{e}^{\pm i\alpha} \tag{51}$$

where

$$\tilde{\tau}_{\rho z_k}^{(1)} = \mathrm{Re}\left[\frac{\sin\varphi - \lambda_k \cos\varphi}{\sqrt{\cos\varphi + \lambda_k \sin\varphi}}\right] \qquad \tilde{\tau}_{\varphi z_k}^{(1)} = \mathrm{Re}\left[\sqrt{\cos\varphi + \lambda_k \sin\varphi}\right]$$

$$\tilde{\tau}_{\rho z_k}^{(2)} = -\frac{\mu_k}{\sqrt{\mu_1 \mu_2}} \cos\varphi\, \mathrm{Re}\left[-i\lambda_k\right] \qquad \tilde{\tau}_{\varphi z_k}^{(2)} = \frac{\mu_k}{\sqrt{\mu_1 \mu_2}} \sin\varphi\, \mathrm{Re}\left[-i\lambda_k\right]$$

$$\left.\begin{aligned} \tilde{\tau}_{\rho z_k}^{(3)} &= \mathrm{Re}\left[(\sin\varphi - \lambda_k \cos\varphi)\Phi_{3k} \mp \sqrt{\cos\varphi + \lambda_k \sin\varphi}\cos\varphi \sin\alpha\right] \\ \tilde{\tau}_{\varphi z_k}^{(3)} &= \mathrm{Re}\left[(\cos\varphi + \lambda_k \sin\varphi)\Phi_{3k} \pm \frac{\sin\varphi - \lambda_k \cos\varphi}{\sqrt{\cos\varphi + \lambda_k \sin\varphi}} \cos\varphi \sin\alpha\right] \end{aligned}\right\} \quad \text{near } B, A = a\mathrm{e}^{\pm i\alpha}.$$

By the use of expressions of the stress field for the curved crack in cylindrically anisotropic materials, the near crack-tip stress fields for the following special cases can be obtained:

(1) *Planar crack in rectilinearly anisotropic materials*

Letting $a \to \infty$, and keeping $a\alpha$ = constant, it follows that

$$\tau_{\gamma z}^{(k)} = \mp \sum_{i=1}^{3} B_i \rho^{s_i} \tilde{\tau}_{\gamma z_k}^{(i)}(\varphi) \quad \gamma = \rho, \varphi, \quad \text{near } B, A = a e^{\pm i\alpha} \tag{52}$$

where $\tilde{\tau}_{\rho z_k}^{(i)}, \tilde{\tau}_{\varphi z_k}^{(i)}, i = 1, 2$ are the same as those for the curved crack.

$$\tilde{\tau}_{\rho z_k}^{(3)} = \tfrac{3}{4}\mathrm{Re}\left[(\sin\varphi - \lambda_k \cos\varphi)\sqrt{\cos\varphi + \lambda_k \sin\varphi}\right] \quad \tilde{\tau}_{\varphi z_k}^{(3)} = \tfrac{3}{4}\mathrm{Re}\left[(\cos\varphi + \lambda_k \sin\varphi)^{3/2}\right]$$

$$B_1 = \lim_{\substack{a\to\infty \\ a\alpha = \text{const}}} A_1 = \frac{\mu_1 \tau_0}{\mu_1 + \mu_2}\sqrt{2a\alpha}\cos\beta$$

$$B_2 = \lim_{\substack{a\to\infty \\ a\alpha = \text{const}}} A_2 = \frac{2\sqrt{\mu_1\mu_2}\,\tau_0}{\mu_1 + \mu_2}\sin\beta$$

$$B_3 = \lim_{\substack{a\to\infty \\ a\alpha = \text{const}}} A_3 = \frac{\mu_1 \tau_0}{\mu_1 + \mu_2}\sqrt{\frac{2}{a\alpha}}\cos\beta.$$

(2) *Curved crack in two isotropic materials*

Letting $\lambda_k = i$, $k = 1, 2$, from the results for anisotropic materials, we have

$$\tau_{\gamma z}^{(k)} = -\sum_{i=1}^{3} A_i \rho^{s_i} \tilde{\tau}_{\gamma z_k}^{(i)}(\varphi) \quad \gamma = \rho, \varphi, \quad \text{near } B, A = a e^{\pm i\alpha} \tag{53}$$

where

$$\tilde{\tau}_{\rho z_k}^{(1)} = \sin\frac{\varphi}{2} \quad \tilde{\tau}_{\varphi z_k}^{(1)} = \cos\frac{\varphi}{2}$$

$$\tilde{\tau}_{\rho z_k}^{(2)} = -\frac{\mu_k}{\sqrt{\mu_1\mu_2}}\cos\varphi \quad \tilde{\tau}_{\varphi z_k}^{(2)} = \frac{\mu_k}{\sqrt{\mu_1\mu_2}}\sin\varphi$$

$$\left.\begin{aligned} \tilde{\tau}_{\rho z_k}^{(3)} &= \frac{3}{4}\left\{\left[\cos\alpha \pm 2\sin\alpha\tan\left(\beta \mp \frac{\alpha}{2}\right)\right]\sin\tfrac{3}{2}\varphi \mp \sin\alpha\cos\tfrac{3}{2}\varphi\right\} \\ \tilde{\tau}_{\varphi z_k}^{(3)} &= \frac{3}{4}\left\{\left[\cos\alpha \pm 2\sin\alpha\tan\left(\beta \mp \frac{\alpha}{2}\right)\right]\cos\tfrac{3}{2}\varphi \pm \sin\alpha\sin\tfrac{3}{2}\varphi\right\} \end{aligned}\right\} \quad \text{near } B, A = a e^{\pm i\alpha}.$$

Introducing the stress intensity factor K_{III}, the leading term in eqns (50) may be written as

$$\tau_{rz}^{(k)} = \frac{K_{\mathrm{III}}}{\sqrt{2\pi\rho}}\mathrm{Re}\left[\frac{1}{\sqrt{\cos\varphi + \lambda_k \sin\varphi}}\right] \quad \tau_{\theta z}^{(k)} = \frac{K_{\mathrm{III}}}{\sqrt{2\pi\rho}}\mathrm{Re}\left[\frac{\lambda_k}{\sqrt{\cos\varphi + \lambda_k \sin\varphi}}\right] \tag{54}$$

where

$$K_{\mathrm{III}} = \frac{2\mu_1}{\mu_1 + \mu_2}\sqrt{a\pi\sin\alpha}\left(\tau_x^{\infty}\cos\frac{\alpha}{2} \pm \tau_y^{\infty}\sin\frac{\alpha}{2}\right) = \sqrt{2\pi}A_1 \quad \text{near } z = a e^{\pm i\alpha} \tag{55}$$

$$\lambda_1 = \left[\frac{C_{45} + i\sqrt{C_{44}C_{55} - C_{45}^2}}{C_{55}}\right]_{(1)} \quad \lambda_2 = i$$

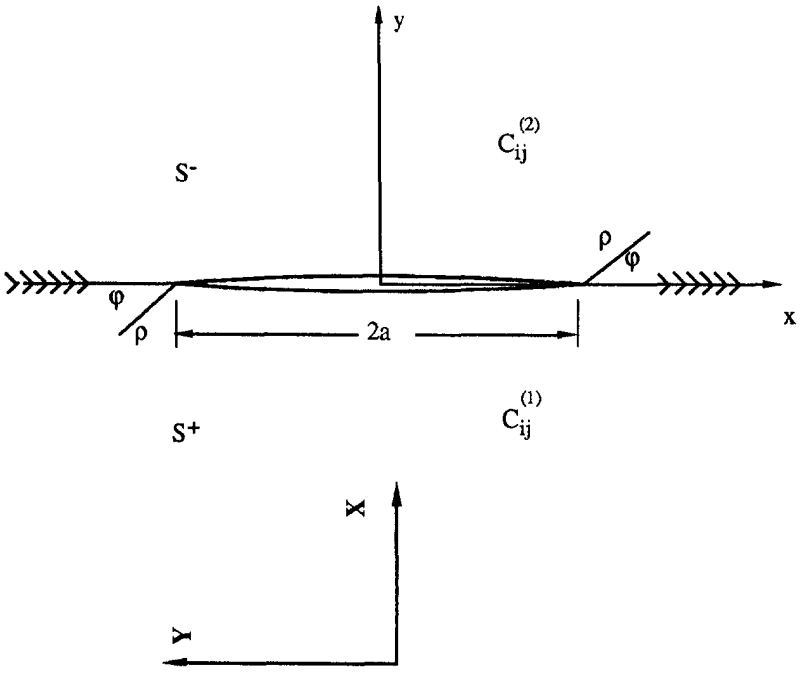

Fig. 2. Geometry and coordinates of interfacial planar crack between rectilinearly anisotropic materials.

$$\mu_1 = [\sqrt{C_{44}C_{55} - C_{45}^2}]_{(1)} \quad \mu_2 = (C_{44})_{(2)} = (C_{55})_{(2)} = G_2$$

and G_2 is the shear modulus of the external material.

If the inner material is isotropic, then $\lambda_1 = i$, the singular terms of eqns (54) are in accord with the results obtained by Tamate and Yamada (1969) and Smith (1969).

4. RESULTS AND DISCUSSION

For the case of a constant surface traction along a crack surface, the stress intensity factor is plotted in Fig. 3 with crack angles ranging from 0 to π. The stress intensity factor increases monotonically as the crack angle increases. When the extent of the interfacial crack approaches complete debond, the stress intensity factor becomes unbound. The ratio of the stress intensity factors between the curved crack and the straight crack with the same crack length is shown in Fig. 3(b). From the figure it can be observed that the stress intensity factor for the curved crack is always greater than that of a straight crack. The angular distribution for the singular term is the same for the surface traction and the prescribed uniform stress at infinity. Figs 4–7 show the stress angular distributions for orthotropic materials and $\gamma = \sqrt{C_{44}/C_{55}}$ ($\lambda = i\gamma$). The angular distributions, $\bar{\tau}_{\rho z}^{(1)}$ and $\bar{\tau}_{\varphi z}^{(1)}$, for three different anisotropy ratios $\gamma = 1$, 2, and 3 are depicted in Fig. 4. The isotropic case with $\gamma = 1$ is plotted for comparison purposes. It is seen that as the anisotropy ratio increases, the gradient of the angular distribution increases and the maximum value of $\bar{\tau}_{\varphi z}^{(1)}$ shifts further from the interface. The second-term expansions for both cases follow simple trigonometric functions and they will not be discussed here. Figures 5–7 describe the angular distribution for the third-term expansion as functions of crack angles with the anisotropy ratio being a parameter. In Fig. 8, comparison of the three-term asymptotic solution with the exact solution and singular solutions at the upper tip B are studied. The singular term solution matches the exact solution as the distance ρ asymptotically approaches the crack tip, while the third-term solution coincides with the exact solution in the much larger region from the crack tip.

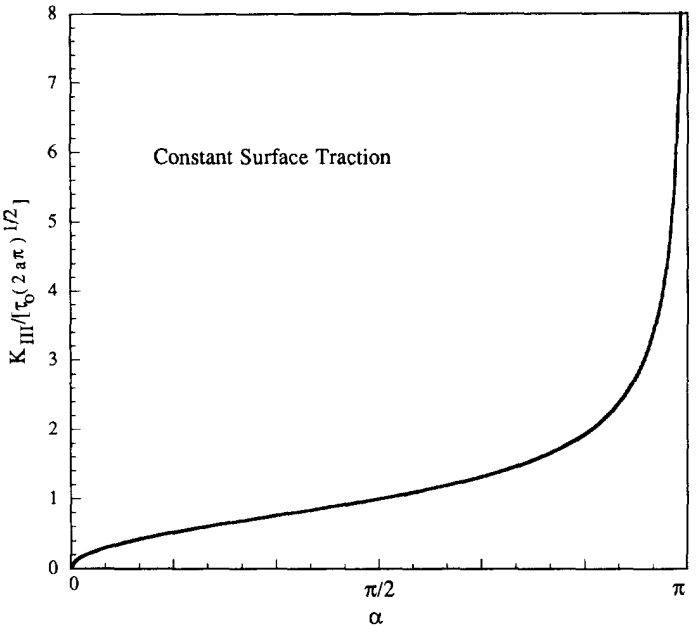

Fig. 3(a). Variation of K_{III} on the crack geometry.

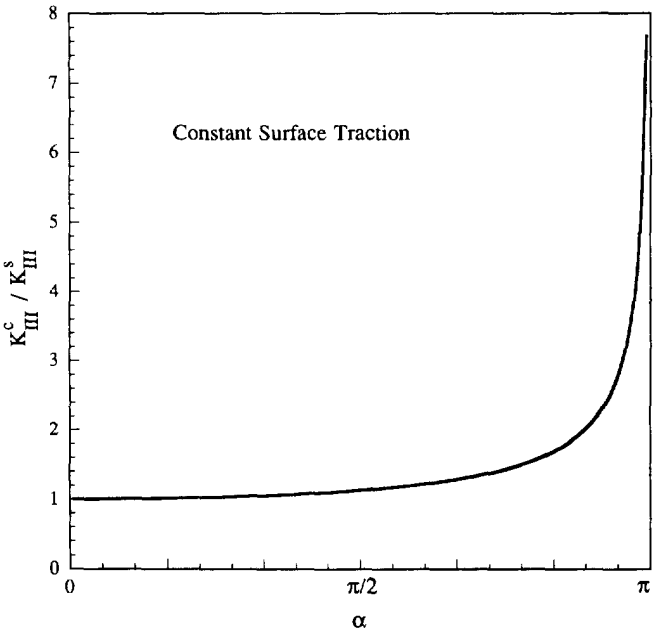

Fig. 3(b). Ratio of stress intensity factor between curved and planar crack.

For the case of prescribed uniform shear stresses at infinity, the crack surface is free of traction and the outer material is isotropic. Fig. 8(a) shows the variation of the stress intensity factor with respect to the crack angle for three different loading angles. The ratio of the stress intensity factor between the curved crack and the straight crack for three different crack angles with identical crack length is shown in Fig. 8(b). Lastly, Figs 9–10 illustrate the stress angular distribution of the third term in the orthotropic material 1. Since the angular distribution varies with the loading angle, in these figures three different loading angles $\beta = 0$, $\pi/4$, and $\pi/2$ are shown. Also, the case of a planar crack is also plotted for comparison. In the figures, two crack angles $\alpha = \pi/4$ and $\pi/2$ for a fixed anisotropic ratio $\gamma = 2$ are taken as examples.

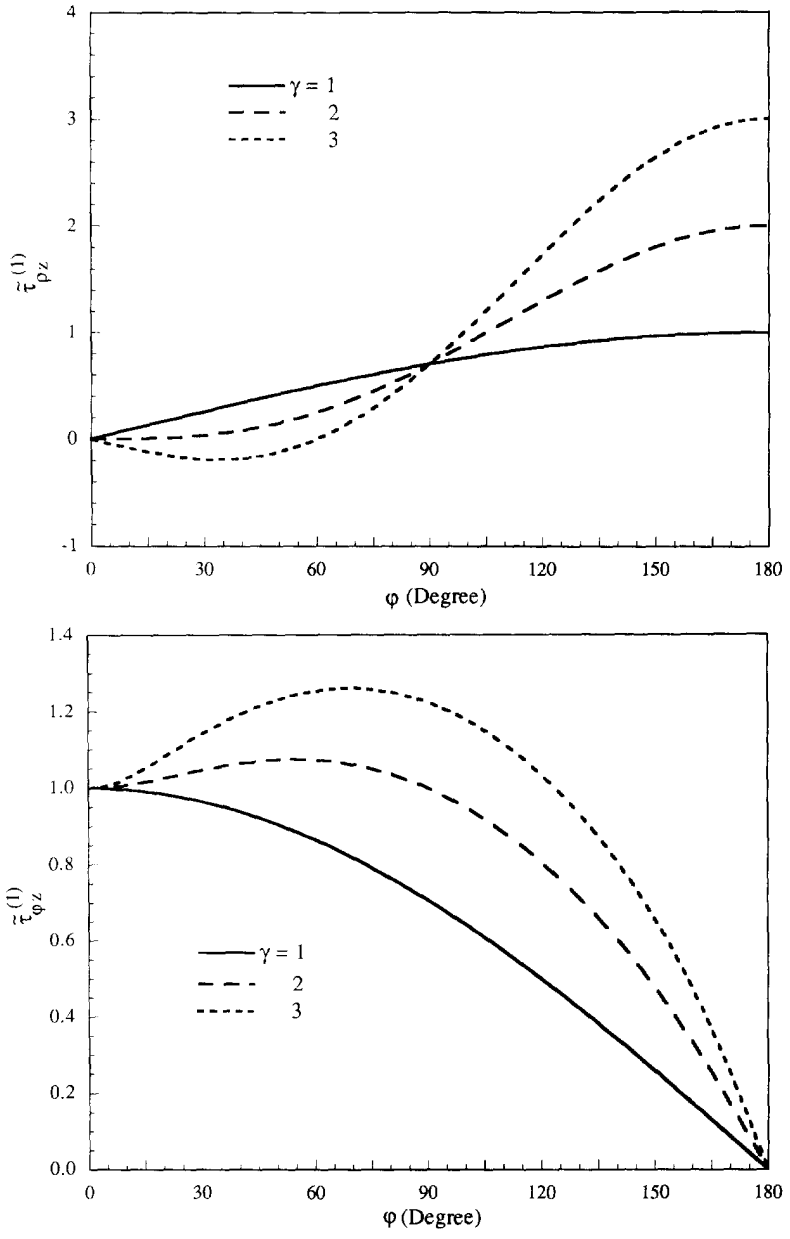

Fig. 4. Stress angular distribution of the leading term for various γ. (a) $\tilde{\tau}_{\rho z}$; (b) $\tilde{\tau}_{\varphi z}$.

5. CONCLUSIONS

The problem of a dissimilar interfacial circular crack in cylindrically anisotropic composites under antiplane shear was studied. A complex variable displacement function, supported by the theory of analytic solutions, was introduced to solve this class of problem in a closed form for some cases. The asymptotic solutions up to the third-term expansion were derived in assessing the role of curvature on the angular distribution of the stresses. The dissimilar interfacial straight crack in rectilinearly anisotropic composites under antiplane shear was also formulated and can be obtained from the curved interfacial crack in cylindrically anisotropic composites as $a \to \infty$. Based on the formulation and numerical results, the following conclusions are drawn:

(1) The inverse square root stress singularity and higher-order stress exponents in the asymptotic expansion of the near crack-tip stress fields are independent of material anisotropy and material properties across the interface.

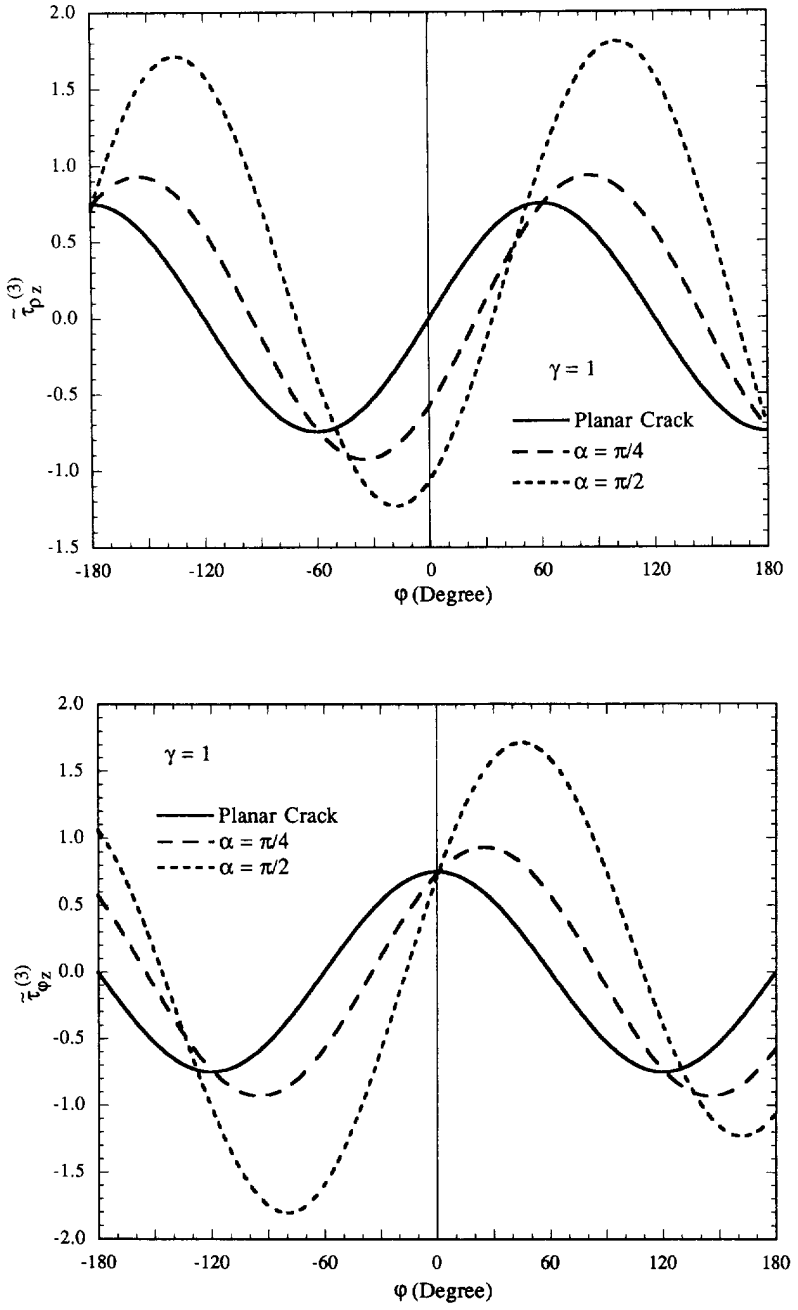

Fig. 5. Stress angular distribution of the third-term under surface traction. (a) $\tilde{\tau}_{\rho z}$; (b) $\tilde{\tau}_{\varphi z}$ for $\gamma = 1$.

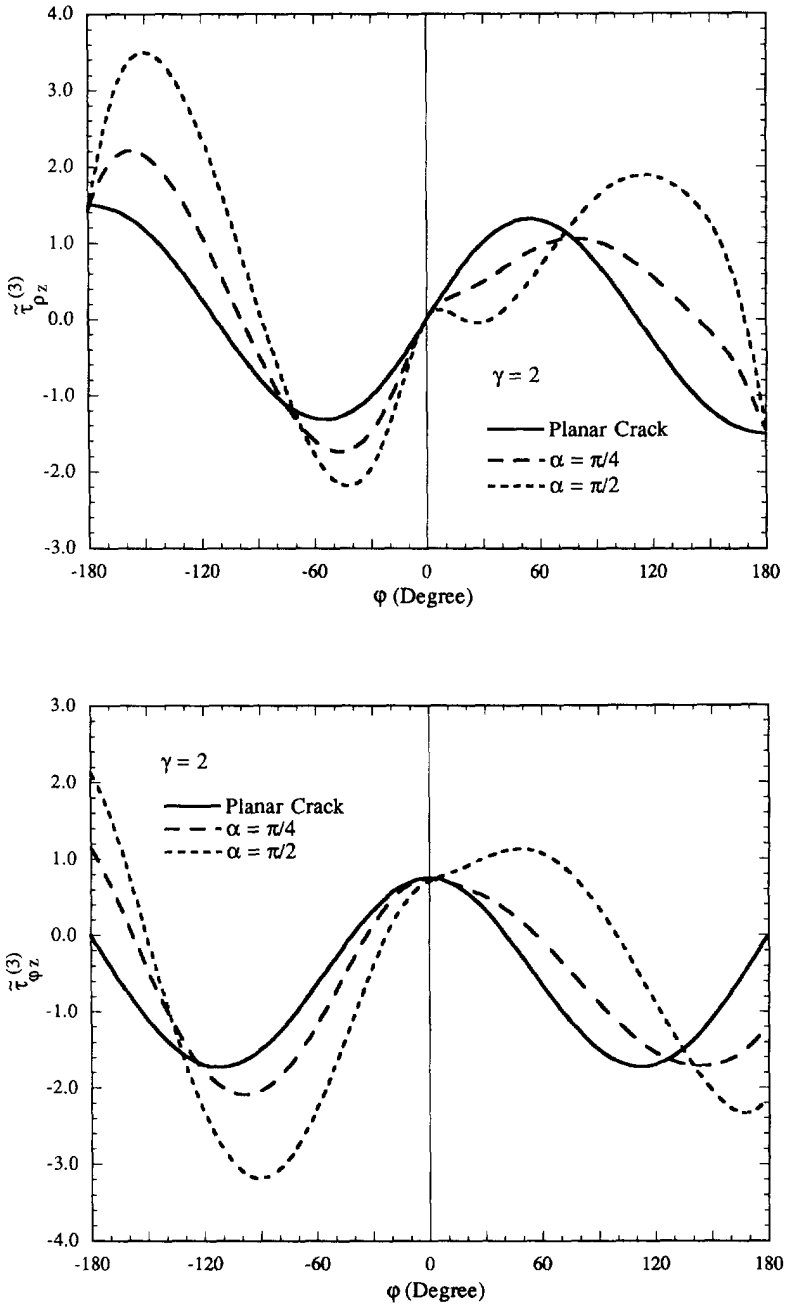

Fig. 6. Stress angular distribution of the third-term under surface traction. (a) $\tilde{\tau}_{\rho z}$; (b) $\tilde{\tau}_{\varphi z}$ for $\gamma = 2$.

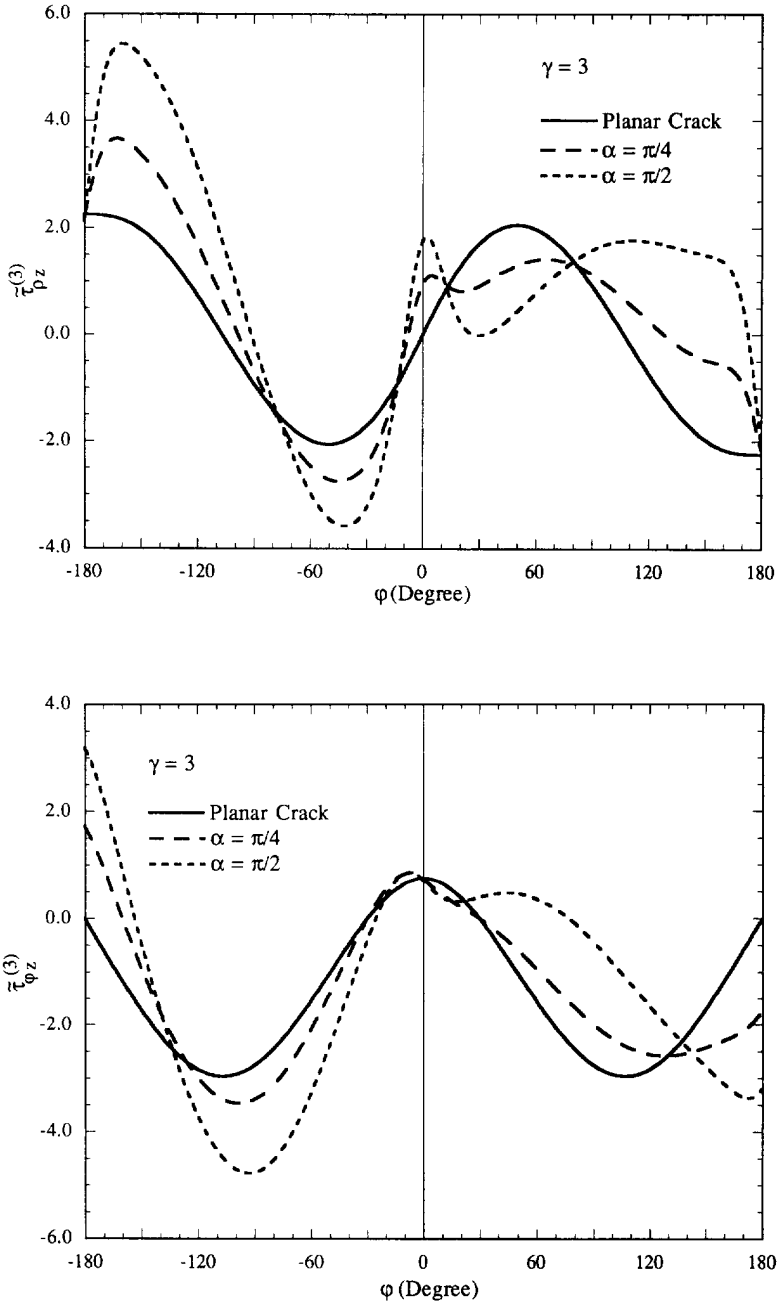

Fig. 7. Stress angular distribution of the third-term under surface traction. (a) $\tilde{\tau}_{\rho z}$; (b) $\tilde{\tau}_{\varphi z}$ for $\gamma = 3$.

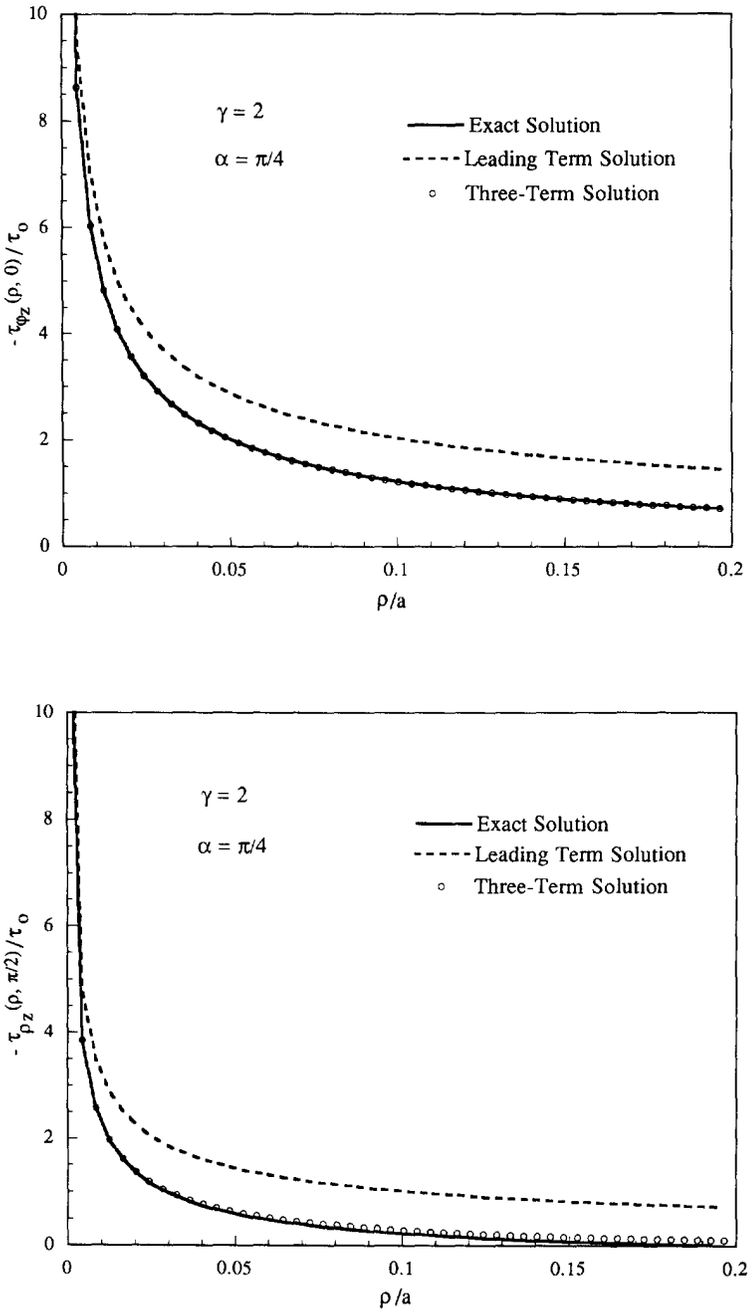

Fig. 8. Comparison of three-term asymptotic solution with exact and leading term solutions. (a) $\tau_{\theta z}(\rho, 0)$; (b) $\tau_{\rho z}(\rho, \pi/2)$.

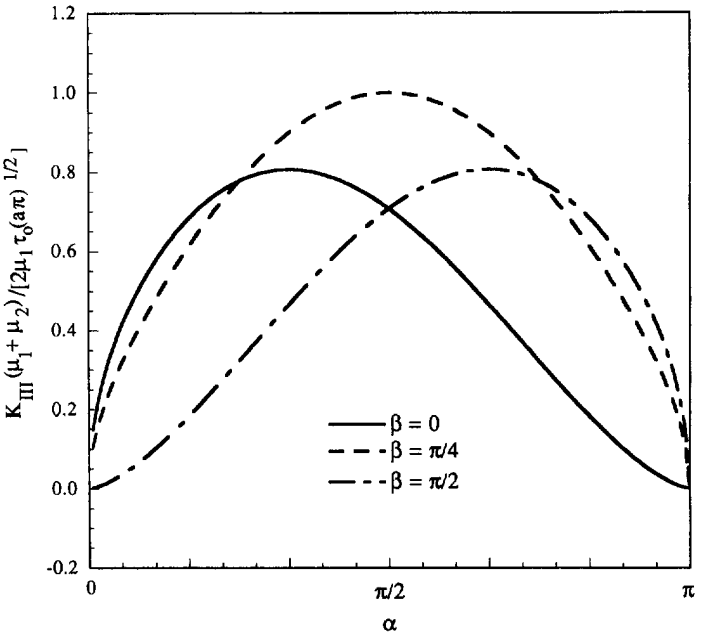

Fig. 9(a). Variation of K_{III} on the loading angle under traction at infinity.

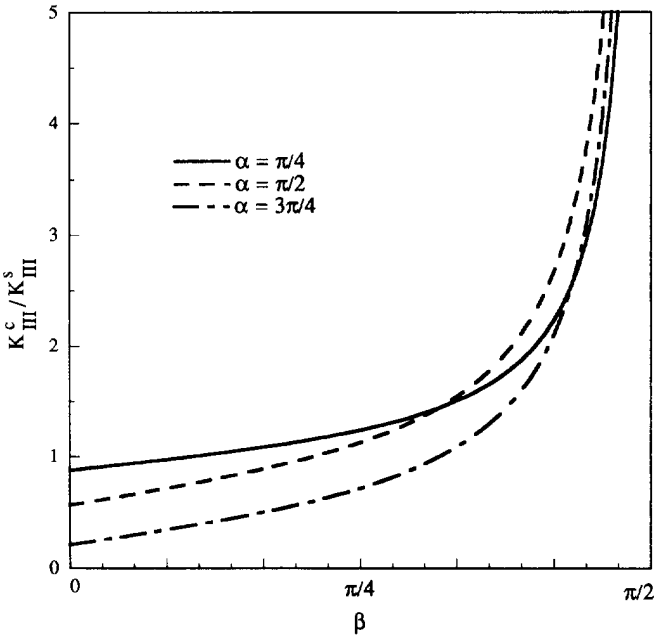

Fig. 9(b). Ratios of stress intensity factor between curved and planar cracks for various crack geometries under traction at infinity.

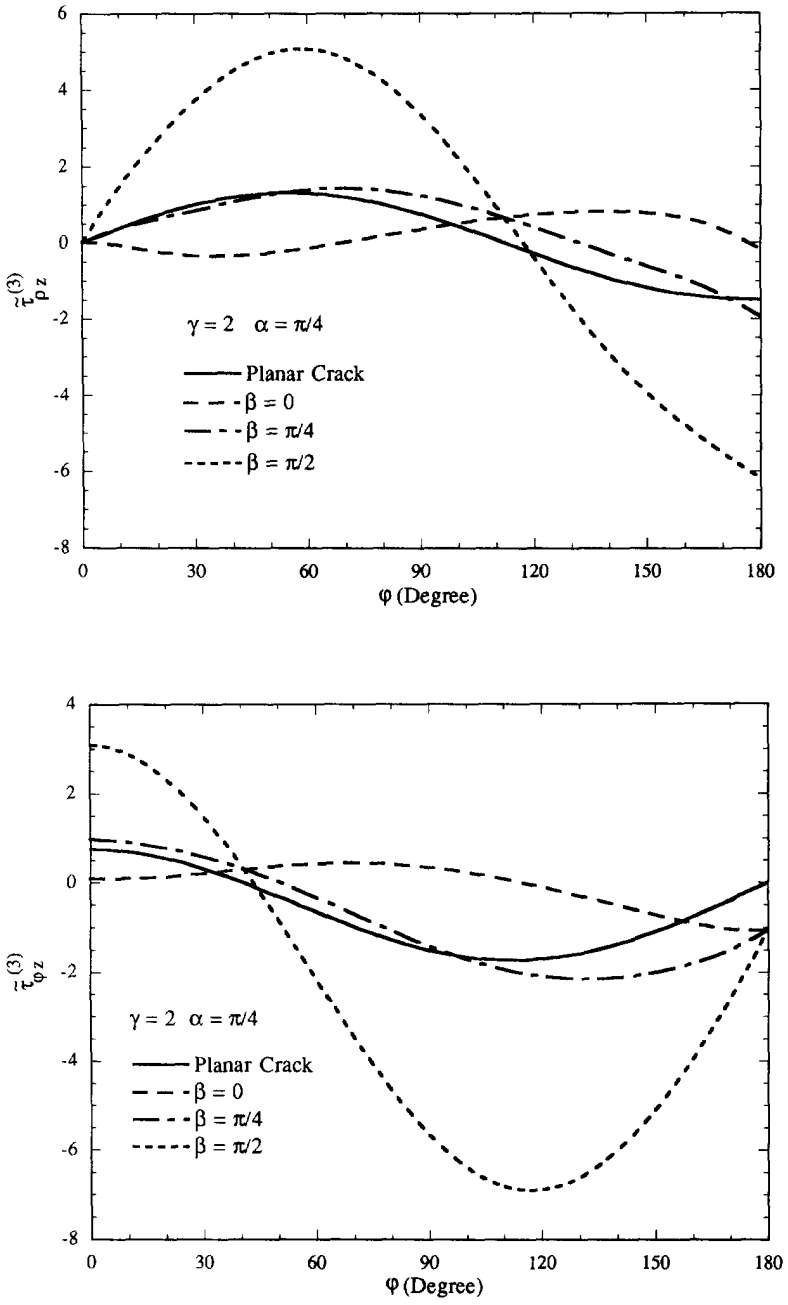

Fig. 10. Stress angular distribution of the third-term under traction at infinity. (a) $\tilde{\tau}_{\rho z}$; (b) $\tilde{\tau}_{\varphi z}$ for $\gamma = 2, \alpha = \pi/4$.

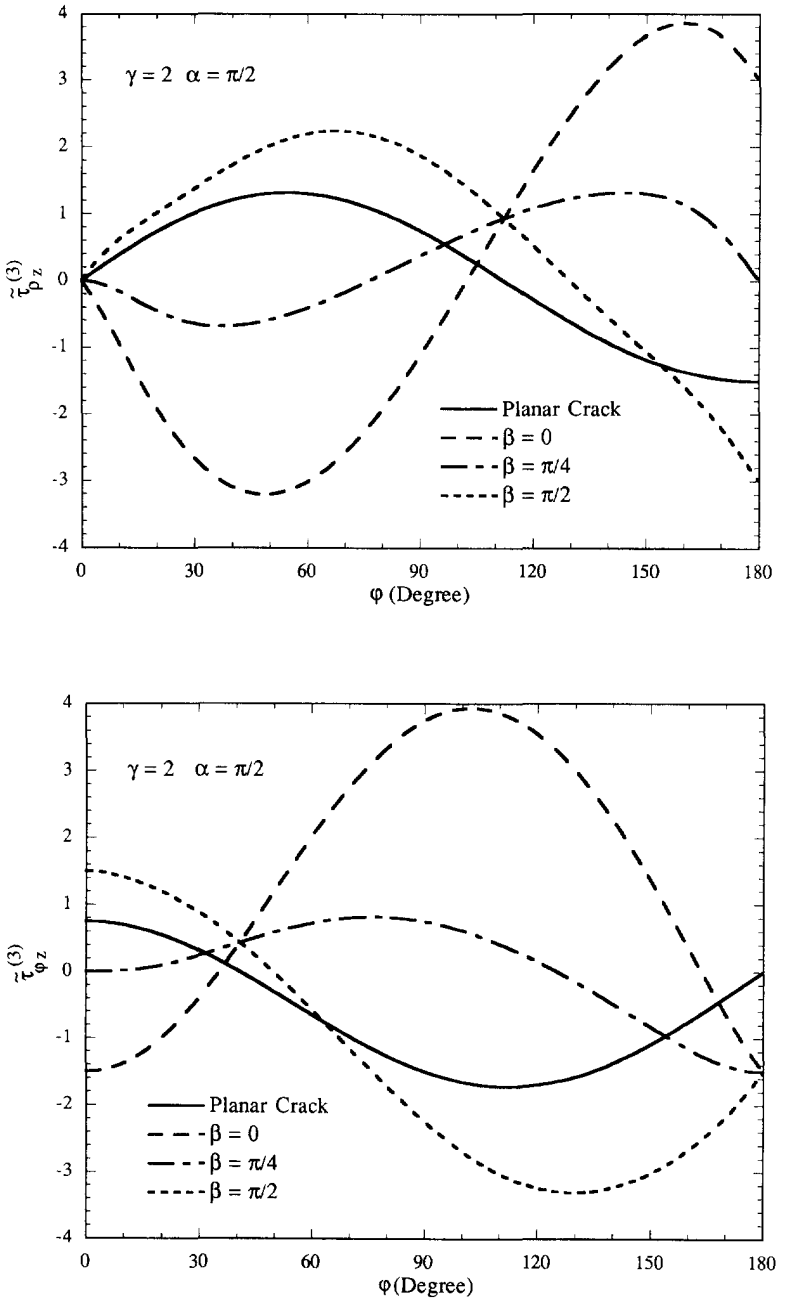

Fig. 11. Stress angular distribution of the third-term under traction at infinity. (a) $\tilde{\tau}_{\rho z}$, (b) $\tilde{\tau}_{\varphi z}$ for $\gamma = 2$, $\alpha = \pi/2$.

(2) The stress intensity factor for the curved crack is greater than that of a straight crack for constant surface traction. In other words, the curvature of the crack enhances the stress intensification near the crack tip.

(3) The asymptotic solutions for the curved crack reveal that although the amplitudes, A_k, ($k = 1,2,3,\ldots$), may be dependent on crack geometry, the stress angular distributions for the first singular term and the second term are independent of the crack geometry. In fact, the angular distribution of the first term only depends on parameter λ_k. The curvature effect on the angular distribution only enters from the third-term. Therefore, the curved crack and the straight crack have identical angular distribution for the first two terms.

(4) The third-term angular distribution of stress may vary with the loading conditions and the crack geometry.

(5) The first three-term asymptotic solution provides accurate stress distributions in a much larger region near the crack tip, while the leading term solution only gives accurate stress distributions in the limit as $r \to 0$.

Acknowledgment This research is supported by the National Science Foundation Grant No. MSS-9202223.

REFERENCES

Choi, S. R. and Earmme, Y. Y. (1990). Analysis of a kinked crack in antiplane shear. *Mech. Mater.* **9,** 195–204.
Choi, S. R. Lee, K. S. and Earmme, Y. Y. (1994). Analysis of a kinked interfacial crack under out-of-plane shear. *ASME J. Appl. Mech.* **61,** 38–44.
Karihaloo, B. L. and Viswanathan, K. (1985). Elastic field of an elliptic inhomogeneity with debonding over an arc. *ASME J. Appl. Mech.* **52,** 91–97.
Lekhnitskii, S. G. (1963). *Theory of Elasticity of an Anisotropic Elastic Body*. Holden-Day, San Francisco.
Muskhelishvili, N. I. (1953). *Some Basic Problems of the Mathematical Theory of Elasticity, 3rd Edition*. English Translation by J. R. Radok, P. Noordhoff and Company, Broningen.
Sih, G. C. (1965). Stress distribution near internal crack tips for longitudinal shear problems. *ASME J. Appl. Mech.* **32,** 51–58.
Sih, G. C. and Chen, E. P. (1981). Cracks in composite materials. In *Mechanics of Fracture*, (Edited by G. C. Sih). Vol. 6, pp. 19–22. Martinus Nijhoff Publishers, The Hague.
Smith, E. (1969). The extension of circular-arc cracks in anti-plane strain deformation. *Int. J. Engng Sci.* **7,** 973–991.
Tamate, O. and Yamada, T. (1969). Stresses in an infinite body with a partially bonded circular cylindrical inclusion under longitudinal shear. *Technology Reports*, Tohoku University, Japan, Vol. 34, No. 1, pp. 161–171.
Teng, H. (1992). Effective longitudinal shear modulus of a unidirectional fiber composite containing interfacial cracks. *Int. J. Solids Structures* **29**(2) 1581–1595.
Teng, H. and Agah-Tehrani, A. (1993). A doubly periodic rectangular array of fiber–matrix interfacial cracks under longitudinal shearing. *ASME J. Appl. Mech.* **60,** 759–762.
Wu, K. C. and Chiu, Y. T. (1991). Antiplane shear interface cracks in anisotropic bimaterials. *ASME J. Appl. Mech.* **58,** 399–403.
Zhang, X. S. (1984). A central crack at the interface between two different media in a rectangular sheet under antiplane shear. *Engng Fract. Mech.* **19**(4) 709–715.

APPENDIX

Straight crack between dissimilar rectilinearly anisotropic materials

Consider a rectilinear anisotropic body to be deformed such that the only nonvanishing displacement component is along the z-axis. The strain–displacement, stress–strain, and equilibrium equation in the absence of body force based on an x–y coordinate system are

$$\gamma_{xz} = \frac{\partial w}{\partial x} \quad \gamma_{yz} = \frac{\partial w}{\partial y} \tag{A.1}$$

$$\tau_{yz} = c_{44}\gamma_{yz} + c_{45}\gamma_{xz} \quad \tau_{xz} = c_{45}\gamma_{yz} + c_{55}\gamma_{xz} \tag{A.2}$$

$$\frac{\partial \tau_{xz}}{\partial x} + \frac{\partial \tau_{yz}}{\partial y} = 0 \tag{A.3}$$

where $w(x, y)$ is the longtudinal displacement, and $\gamma_{\beta z}$ and $\tau_{\beta z}$ are strain and stress components respectively c_{ij} are stiffness coefficients. Using eqns (A.1) and (A.2), the equilibrium equation (A.3) yields

$$c_{55}\frac{\partial^2 w}{\partial x^2} + 2c_{45}\frac{\partial^2 w}{\partial x \partial y} + c_{44}\frac{\partial^2 w}{\partial y^2} = 0. \tag{A.4}$$

A general solution for eqn (A.4) can be expressed as

$$w(x, y) = 2\,\mathrm{Re}[W(z_3)] \tag{A.5}$$

where $z_3 = x + sy$, the constants s are roots of the following algebraic characteristic equation

$$c_{44}s^2 + 2c_{45}s + c_{55} = 0 \tag{A.6}$$

and s is chosen as

$$s = [-c_{45} + i\sqrt{c_{44}c_{55} - c_{45}^2}]/c_{44}$$

with $\mathrm{Im}[s] \neq 0$. It is expedient to define

$$\Phi(z_3) = i\sqrt{c_{44}c_{55}-c_{45}^2}\,\frac{\mathrm{d}W(z_3)}{\mathrm{d}z_3} \tag{A.7}$$

so that the shear stresses may be simply written as

$$\tau_{yz} = 2\,\mathrm{Re}\,[\Phi(z_3)] \quad \tau_{xz} = -2\,\mathrm{Re}\,[s\Phi(z_3)] \tag{A.8}$$

and

$$\frac{\partial w}{\partial x} = -\frac{i}{\mu}[\Phi(z_3)-\bar{\Phi}(\bar{z}_3)] \tag{A.9}$$

where $\mu = \sqrt{c_{44}c_{55}-c_{45}^2}$.

Consider a crack of length $2a$ lying along the interface of two anisotropic elastic solids as shown in Fig. 2. Further, let equal and opposite known tractions $\tau(x)$ be applied to each face of the crack. Then boundary conditions along $y = 0$ are

$$\frac{\partial w^{(1)}}{\partial x} = \frac{\partial w^{(2)}}{\partial x} \quad \tau_{yz}^{(1)} = \tau_{yz}^{(2)} \quad \text{on } y = 0, \quad |x| > a \tag{A.10}$$

$$\tau_{yz}^{(1)} = \tau(x) \quad \tau_{yz}^{(2)} = \tau(x) \quad \text{on } y = 0, \quad |x| < a. \tag{A.11}$$

Here, and in the sequel, the superscripts and subscripts 1 and 2 refer to the quantities associated with the materials occupying the lower and upper half planes respectively. From eqns (A.8b) and (A.9), eqn (A.10) leads to

$$\begin{aligned} &\frac{1}{\mu_1}[\Phi_1(z)-\bar{\Phi}_1(\bar{z})] = \frac{1}{\mu_2}[\Phi_2(z)-\bar{\Phi}_2(\bar{z})] \\ &\Phi_1(z)+\bar{\Phi}_1(\bar{z}) = \Phi_2(z)+\bar{\Phi}_2(\bar{z}) \end{aligned} \quad \text{on } y = 0, \quad |x| > a$$

which may be rewritten in the form

$$\begin{aligned} &\frac{1}{\mu_1}\Phi_1(z)-\frac{1}{\mu_2}\bar{\Phi}_2(\bar{z}) = \frac{1}{\mu_2}\Phi_2(z)+\frac{1}{\mu_1}\bar{\Phi}_1(\bar{z}) \\ &\Phi_1(z)-\bar{\Phi}_2(\bar{z}) = \Phi_2(z)-\bar{\Phi}_1(\bar{z}) \end{aligned} \quad \text{on } y = 0, \quad |x| > a.$$

Thus, if we define

$$\begin{aligned} &\frac{1}{\mu_1}\Phi_1(z)+\frac{1}{\mu_2}\bar{\Phi}_2(\bar{z}) \equiv \Psi(z) \quad z\in S^- \\ &\frac{1}{\mu_2}\Phi_2(z)+\frac{1}{\mu_1}\bar{\Phi}_1(\bar{z}) \equiv \Psi(z) \quad z\in S^+ \\ &\Phi_1(z)-\bar{\Phi}_2(\bar{z}) \equiv \Theta(z) \quad z\in S^- \\ &\Phi_2(z)-\bar{\Phi}_1(\bar{z}) \equiv \Theta(z) \quad z\in S^- \end{aligned} \tag{A.12}$$

then the displacements and stress are continuous across the interface. $\Psi(z)$ and $\Theta(z)$ are analytic functions in x–y plane cut along $y = 0$, $|x| < a$, S^- and S^+ are the regions of the half planes $y > 0$ and $y < 0$, respectively. Solving eqn (A.12) for $\Phi_1(z)$ and $\Phi_2(z)$, we have

$$\begin{aligned} &\Phi_1(z) = \frac{\mu_1\mu_2}{\mu_1+\mu_2}\left[\Psi(z)+\frac{\Theta(z)}{\mu_2}\right], \quad \bar{\Phi}_2(\bar{z}) = \frac{\mu_1\mu_2}{\mu_1+\mu_2}\left[\Psi(z)-\frac{\Theta(z)}{\mu_1}\right] \quad z\in S \\ &\Phi_2(z) = \frac{\mu_1\mu_2}{\mu_1+\mu_2}\left[\Psi(z)+\frac{\Theta(z)}{\mu_1}\right], \quad \bar{\Phi}_1(\bar{z}) = \frac{\mu_1\mu_2}{\mu_1+\mu_2}\left[\Psi(z)-\frac{\Theta(z)}{\mu_2}\right] \quad z\in S^+ \end{aligned} \tag{A.13}$$

Substituting eqn (A.13) into the remaining condition (A.11), we have

$$\begin{aligned} &\Psi^-(z)+\Psi^+(z)+\frac{1}{\mu_2}[\Theta^-(z)-\Theta^+(z)] = \tau(z)\frac{\mu_1+\mu_2}{\mu_1\mu_2} \\ &\Psi^-(z)-\Psi^+(z)-\frac{1}{\mu_1}[\Theta^-(z)-\Theta^+(z)] = \tau(z)\frac{\mu_1+\mu_2}{\mu_1\mu_2} \end{aligned} \quad \text{on } y = 0, |x| < a \tag{A.14}$$

that is

$$\Theta^{+}(x)-\Theta^{-}(x)=0 \quad \Psi^{+}(x)+\Psi^{-}(x)=\tau(x)\frac{\mu_1+\mu_2}{\mu_1\mu_2} \quad \text{on } y=0, \quad |x|<a \tag{A.15}$$

where the superscripts + and − stand for the boundary values of the functions as z approaches the boundary from S^{+} and S^{-} respectively. The two unknown functions $\Psi(z)$ and $\Theta(z)$ are governed by eqns (A.15), which are a pair of Hilbert problems. The solutions of eqns (A.15) which have been given by Muskhelishvili (1953) can be expressed as

$$\Theta(z)=P(z) \tag{A.16}$$

$$\Psi(z)=\frac{1}{2\pi i}\frac{\mu_1+\mu_2}{\mu_1\mu_2}\chi_0(z)\int_L\frac{\tau(t)\,\mathrm{d}t}{\chi_0^{+}(t)(t-z)}+\chi_0(z)R(z) \tag{A.17}$$

where $P(z)$ and $R(z)$ are holomorphic in the whole plane except at the origin and infinity; L is the line $|x|<a$, $y=0$; and

$$\chi_0(z)=(z-a)^{-1/2}(z+a)^{-1/2}. \tag{A.18}$$

If the body is taken to infinity in extent and the stresses are assumed to vanish at infinity. Then for the special case of $\tau(z)=-\tau_0=$ constant, the solutions to eqns (A.16) and (A.17) are

$$\Psi(z)=-\frac{\mu_1+\mu_2}{2\mu_1\mu_2}\tau_0\left[1-\frac{z}{\sqrt{z^2-a^2}}\right] \quad \Theta(z)=0. \tag{A.19}$$

Using eqns (A.13) and (A.19), and replacing the argument z by z_k, we have

$$\begin{aligned}\Phi_1(z_3)&=-\frac{\tau_0}{2}\left[1-\frac{z_3}{\sqrt{z_3^2-a^2}}\right] \quad z_3\in S^{+}\\ \Phi_2(z_3)&=-\frac{\tau_0}{2}\left[1-\frac{z_3}{\sqrt{z_3^2-a^2}}\right] \quad z_3\in S^{-}.\end{aligned} \tag{A.20}$$

Note that because all boundary conditions are satisfied by $\Phi_j(z_3)$, $\Phi_j(z_3)$ are the solutions for this problem. Expanding $\Phi_1(z_3)$ and $\Phi_2(z_3)$ for small values of ρ from the crack tip, using eqn (A.8), the first three-term asymptotic expansions of the crack-tip stress field can be expressed as

$$\begin{aligned}\tau_{xz}^{(k)}&=\frac{K_{\mathrm{III}}}{\sqrt{2\pi\rho}}\mathrm{Re}\left[\frac{1}{\sqrt{\cos\varphi+s_k\sin\varphi}}\right]-\tau_0+\tau_0\sqrt{\frac{\rho}{2a}}\frac{3}{4}\mathrm{Re}\left[\sqrt{\cos\varphi+s_k\sin\varphi}\right]\\ \tau_{yz}^{(k)}&=\frac{K_{\mathrm{III}}}{\sqrt{2\pi\rho}}\mathrm{Re}\left[\frac{-s_k}{\sqrt{\cos\varphi+s_k\sin\varphi}}\right]-\tau_0\,\mathrm{Re}\left[-s_k\right]+\tau_0\sqrt{\frac{\rho}{2a}}\frac{3}{4}\mathrm{Re}\left[-s_k\sqrt{\cos\varphi+s_k\sin\varphi}\right]\end{aligned} \tag{A.21}$$

where

$$K_{\mathrm{III}}=\tau_0\sqrt{\pi a}$$

Using the stress transformation

$$\left.\begin{aligned}\tau_{yz}&=\mp\tau_{xz}\sin\varphi\mp\tau_{yz}\cos\varphi\\ \tau_{\theta z}&=\mp\tau_{xz}\cos\varphi\pm\tau_{yz}\sin\varphi\end{aligned}\right\} \quad \text{near } z=\mp a \tag{A.22}$$

the expansion of the crack-tip stress field can be rewritten in the form

$$\left.\begin{aligned}
\tau_{yz} &= \mp \frac{K_{III}}{\sqrt{2\pi\rho}} \operatorname{Re}\left[\frac{\sin\varphi - s_k\cos\varphi}{\sqrt{\cos\varphi + s_k\sin\varphi}}\right] \pm \tau_0 \operatorname{Re}\left[\sin\varphi - s_k\cos\varphi\right] \\
&\quad \mp \tau_0 \sqrt{\frac{\rho}{2a}}\frac{3}{4} \operatorname{Re}\left[\sqrt{\cos\varphi + s_k\sin\varphi}(\sin\varphi - s_k\cos\varphi)\right] \\
\tau_{xz} &= \mp \frac{K_{III}}{\sqrt{2\pi\rho}} \operatorname{Re}\left[\sqrt{\cos\varphi + s_k\sin\varphi}\right] \pm \tau_0 \operatorname{Re}\left[\cos\varphi + s_k\sin\varphi\right] \\
&\quad \mp \tau_0 \sqrt{\frac{\rho}{2a}}\frac{3}{4} \operatorname{Re}\left[(\cos\varphi + s_k\sin\varphi)^{3/2}\right]
\end{aligned}\right\} \quad \text{near } z = \mp a. \tag{A.23}$$

In order to compare the distribution between the curved and planar crack, the X–Y coordinate system shown in Fig. 1 is exhibited in Fig. 2. The stress–strain relation based on this X–Y coordinate can be written as

$$\begin{aligned}
\tau_{YZ} &= C_{44}\frac{\partial W}{\partial Y} + C_{45}\frac{\partial W}{\partial X} \\
\tau_{XZ} &= C_{45}\frac{\partial W}{\partial Y} + C_{55}\frac{\partial W}{\partial X}.
\end{aligned} \tag{A.24}$$

Since the relation in terms of the original local x–y coordinate system is given by eqn (A.2), it follows from the stress and coordinate transformation that

$$C_{44} = C_{55}, \quad C_{55} = C_{44}, \quad C_{45} = -C_{45}$$

Therefore

$$s_k = \left(\frac{-C_{45} + i\sqrt{C_{44}C_{55} - C_{45}^2}}{C_{44}}\right)_k = \left(\frac{C_{45} + i\sqrt{C_{44}C_{55} - C_{45}^2}}{C_{55}}\right)_k = \lambda_k. \tag{A.25}$$

By replacing s_k by λ_k in eqns (A.23), eqns (A.23) completely coincide with eqns (34) which are obtained from the case of curved crack as $a \to \infty$. Note that $2a\alpha$ in eqns (34) is the length of the crack.